Received 31 October 2019; revised 12 January 2020; accepted 2 February 2020. Date of publication 23 January 2020; date of current version 3 March 2020.

Digital Object Identifier 10.1109/OJAP.2020.2972842

An Energy-Synchronous Direct Antenna Modulation Method for Phase Shift Keying

KURT SCHAB [1] (Member, IEEE), DANYANG HUANG [2] (Student Member, IEEE), AND JACOB J. ADAMS [2] (Senior Member, IEEE)

[1]Department of Electrical and Computer Engineering, Santa Clara University, Santa Clara, CA 95053 USA
[2]Department of Electrical and Computer Engineering, Antennas and Electromagnetics Laboratory, North Carolina State University, Raleigh, NC 27606 USA
CORRESPONDING AUTHOR: K. SCHAB (e-mail: kschab@scu.edu)

This work was supported by DARPA under Grant D16AP00033. The work of Kurt Schab was supported by the Intelligence Community Postdoctoral Research Fellowship Program.

ABSTRACT A novel scheme for transmitting broadband phase shift keyed signals from electrically small antennas using energy-synchronous direct antenna modulation is described. We outline fundamental operating principles of the method and experimentally compare its performance to that of a conventional band-limited transmit antenna with the same electrical size and radiation efficiency. Transmitted waveforms are analyzed in the time domain both at RF and baseband. Results show significant increases in signal quality, suggesting a larger effective transmit bandwidth and greater potential throughput when the proposed direct antenna modulation scheme is used.

INDEX TERMS Electrically small antennas, direct modulation, antenna measurements, phase shift keying, time-varying circuits.

I. INTRODUCTION

ANTENNAS face fundamental limits in their minimum radiation Q-factor (and hence, maximum bandwidth-efficiency product) as their electrical size decreases, e.g., the well-known Chu bound for spherical shells [1]. This makes transmitting wideband signals difficult using electrically small antennas because the signals are inherently bandlimited by the undesired bandpass nature of the antenna's impedance match. This bandwidth limitation can be circumvented to some extent by reducing the antenna's efficiency with resistive loading [2], [3], but this is not a desirable solution for most transmit applications.

Over the past several decades, a number of authors have proposed methods using time variant antennas and matching networks to circumvent the bandwidth limitations of electrically small, high Q-factor antennas without reducing efficiency, e.g., [4]–[7]. Transmission schemes that rely on time variant modulation of the antenna or matching network are referred to as direct antenna modulation (DAM). The more promising of these schemes function by storing and releasing energy in the antenna and matching network in synchronization with the digital waveform being transmitted to facilitate rapid transitions between different symbol states. Consequently, another characteristic of these schemes is that they must be tailored for the particular modulation being transmitted. Thus far, nearly all reported results are for on-off keying or frequency shift keying schemes. While one report of phase shift keying using DAM exists [8], the system is designed for near field communication and only circuit simulations are reported.

In this paper we describe, analyze, and measure the radiated far field behavior of a direct antenna modulation-based transmitter for phase shift keying. Though we demonstrate specific cases of binary phase shift keying (BPSK) and quadrature phase shift keying (QPSK) in this paper, the proposed method is capable of producing arbitrary phase shifts at high baud rate. To elucidate the relative performance of the DAM scheme compared to a linear time invariant (LTI) transmit antenna, identical antennas and matching networks are compared while operating in both DAM and LTI modes for all cases studied.

The paper is organized as follows. First, the effects of narrow antenna bandwidth on a broadband phase shift keyed (PSK) signal are examined. Next, the principle of operation of the direct antenna modulation PSK (DAM PSK) scheme is explained. Finally, details of the far

field characterization are described and the results are analyzed.

II. SIGNAL CHARACTERISTICS OF CONVENTIONAL NARROWBAND PSK TRANSMITTERS

Conventional LTI transmitting antennas distort broadband signals that greatly exceed their impedance bandwidth. Consider a PSK signal with M symbol states (e.g., $M = 4$ for quadrature phase shift keying, QPSK) denoted by the phases $\{\phi_i\}$ being transmitted by an electrically small antenna. If a matched single-resonance circuit model for the antenna is adopted [9], the transition of the radiated field between symbol phase states ϕ_1 and ϕ_2 at time $t = 0$ takes the form

$$E_{\text{rad}}(t) \sim \cos(\omega_0 t + \phi_1)\mathrm{e}^{-\alpha t} + \cos(\omega_0 t + \phi_2)\left(1 - \mathrm{e}^{-\alpha t}\right) \quad (1)$$

where $\alpha = Q^{-1}\omega_0$ is a time constant related to the antenna's Q-factor, and thus proportional to its impedance bandwidth [10].

Thus, the exponential transitions between symbol states are due to the slow charging and discharging of uniquely phased oscillations and are the time-domain manifestation of the bandlimited nature of electrically small antennas. Long transition times associated with very narrowband systems lead to high distortion [11], problematic intersymbol interference, and decreased noise tolerance. All of these factors decrease communication link performance.

Throughout this paper the symbol rate of a PSK signal is described by the integer number N of carrier cycles per symbol. As N is decreased, the signal bandwidth increases as $1/N$ and narrowband conventional transmitters will exhibit increased signal distortion.

III. ENERGY-SYNCHRONOUS PSK SCHEME

To avoid the aforementioned limitations imposed by a conventional narrowband transmitter, we propose the following technique based on direct antenna modulation (DAM). The core concepts of this method are adapted from an energy-synchronous technique for on-off-keying [5], [12], [13]. The key element of that technique (discussed in detail in [13]) is the use of a precisely-synchronized switched matching network to capture and release electric energy on the antenna structure to facilitate rapid transitions between a radiating and non-radiating state, thus avoiding detrimental charging and discharging times similar to those appearing in (1). In on-off keying, the radiating and non-radiating states form the two symbol states. Here, we adapt the method to facilitate transitions between symbols of constant amplitude but varying phase. The following scheme shares basic similarities with the method described in [8], though our approach relies only on a single synchronized switch for arbitrary order PSK, uses the capacitance of a small dipole antenna itself for energy storage (rather than an external capacitor bank), and is designed for far-field communications.

The circuit schematic for the proposed DAM PSK system, shown in Figure 1, is identical to that used for OOK in [13]. A small dipole antenna is tuned to resonance at a carrier

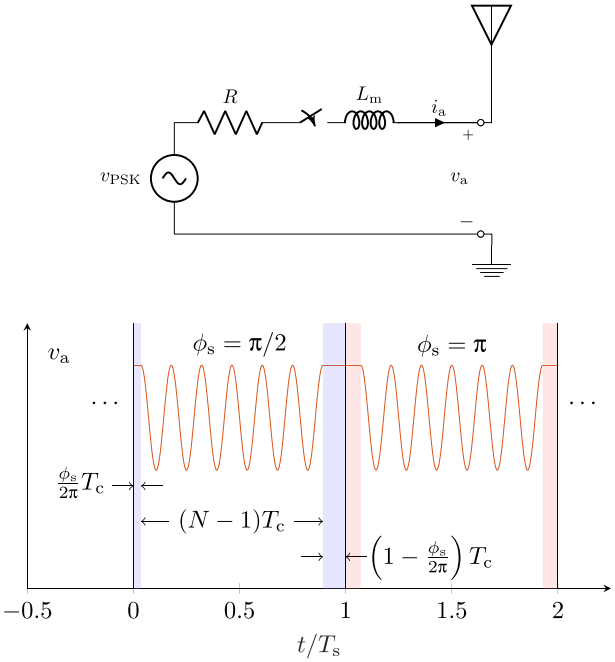

FIGURE 1. Ideal schematic of the proposed DAM PSK transmitter (top) and schematic of lead and lag periods within a symbol transition (bottom).

frequency f_{c} by an appropriate inductance L_{m}. The signal voltage source v_{PSK} is matched to the tuned antenna's input resistance at resonance and connected to the antenna via a single-pole-single-throw (SPST) switch. The system is assumed to have been previously driven to steady state oscillation with the switch in the closed position. If the switch is opened at the instant the antenna terminal voltage v_{a} is maximum, current immediately stops flowing at the antenna terminals and potential energy is trapped on the antenna in the form of opposing charges separated on the two arms of the dipole. With the exception of predictable second-order transient effects [14], this results in near instantaneous suspension of radiation from electrically small dipole antennas, regardless of particular geometry [12].

While holding stored charge and radiation suspended, the antenna can, in principle, be held in a static state indefinitely. In DAM OOK, this fact is used to generate "off" bits with no radiation. Here we use this moment of suspended radiation to lag the antenna by a time corresponding to the desired phase ϕ_{s} of the next symbol to be transmitted. Lags of this kind are shown as shaded regions in Figure 1. During this time, the source v_{PSK} also changes its phase according to the symbol phase. Closing the switch at the instant the source voltage v_{PSK} is zero replicates the first-order initial conditions on the voltages and currents that were in place at the time the switch was opened. Under this properly synchronized condition, radiation resumes near-instantaneously with the desired symbol phase. We transmit the carrier for $N - 1$ carrier cycles and again open the switch at the instant the antenna terminal voltage v_{a} is maximum. This lag is maintained during the $1 - \phi_{\text{s}}/2\pi$ cycles remaining in the

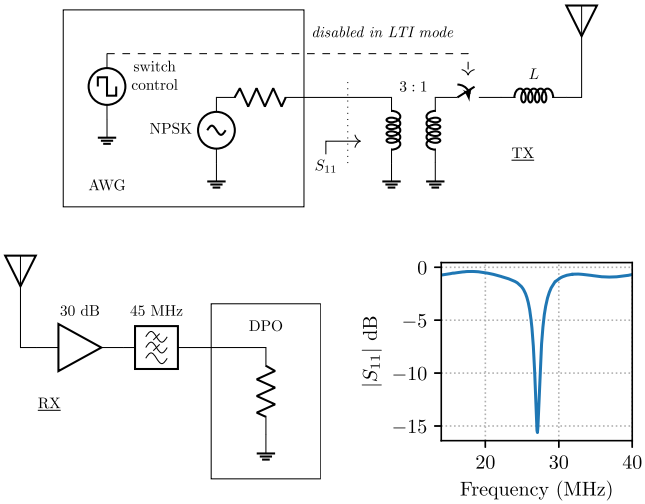

FIGURE 2. Schematic of experimental transmitter (top), receiver (bottom left). Also shown is the tuned transmitter reflection coefficient as seen in LTI mode (bottom right).

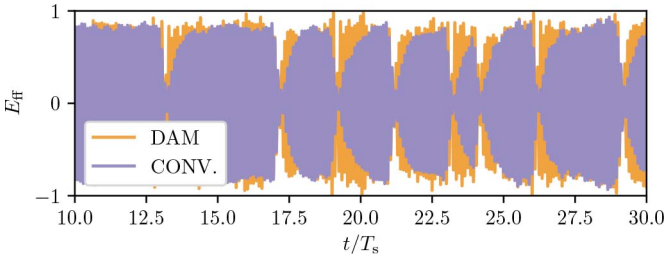

FIGURE 3. A portion of the received time domain signal when transmitting a BPSK PRBS with $N = 10$. Time axis is scaled by symbol length T_{S}.

N-cycle symbol[1] and is joined with the first phasing lag of the following symbol. The scheme can easily be modified to avoid unnecessary lead and lag periods between identical consecutive symbols (same symbol correction, SSC).

IV. FAR FIELD MEASUREMENTS

A. EXPERIMENTAL SETUP

To test the proposed PSK scheme in a far field radiation environment, a transmitter and receiver are set up in an open area on North Carolina State University's campus in an identical manner to that used to evaluate a DAM on-off-key system in [13]. A schematic of the experimental system is shown in Fig. 2. The transmitting antenna is an electrically-short 0.94 m tall monopole antenna (height of 0.085λ at carrier frequency 27.12 MHz, $Z_{\text{in}} = 17 - \text{j}550\ \Omega$) tuned to resonance at 27.12 MHz using a series variable inductance and matched with a 3:1 transformer. The receiving quarter-wave monopole antenna is connected to a lowpass filter (KR Electronics, KR2805) and a 30 dB low-noise amplifier (Minicircuits LNA-530) followed by a 4 GHz oscilloscope (Tektronix DPO70404C). The antennas are selected so that the transmit antenna's 10 dB return loss bandwidth (2.7%), see Fig. 2, is much narrower than the signal first-null fractional bandwidth (20, 40, 66% for PSK with $N = 10,\ 5,\ 3$, respectively) as well as the receive antenna's bandwidth (11.4%). Both antennas are supported by PVC masts and eight radials are used to improve the ground plane performance. A CMOS-based reflective switch (Analog Devices ADG902) modulates the series connection at the antenna's port to implement DAM PSK according to Fig. 1. An arbitrary waveform generator (AWG, Tektronix AWG70002A) produces both the RF carrier and baseband switch control signals. Because the closed switch still adds series loss of approximately 5 Ω to the system and thus slightly broadens the transmitter's impedance bandwidth, it is left in place for both LTI and DAM modes to enable fair comparison of transmission efficacy. The transmitter bandwidth listed is that with the switch in place. In LTI mode, the switch is held in the closed state during the entire transmission of a 256-bit pseudorandom bit sequence (PRBS) produced by the AWG. When running in DAM mode, the PRBS is again produced by the AWG while the dynamic switch control as described in Section III is used to toggle the series switch connection. The transmissions are repeated 70 times, time-aligned, and averaged to create a very high signal-to-noise ratio measurement. The measured RF data is then processed in conjunction with a channel sounding chirp to remove unintentional multipath and receiver effects.[2] Note that in this configuration, both DAM and conventional modes radiate with identical continuous wave radiation efficiency.

B. EXPERIMENTAL RESULTS

In the first experiment, a wideband binary PSK (BPSK, $M = 2$) signal is transmitted through the electrically small transmit antenna when the antenna was operated in both LTI and DAM modes. Several data rates ($N = 10$, 5, and 3) are used, and Fig. 3 shows the time domain characteristics of a portion of the signal for $N = 10$. During the transitions between two different bits (bit "1" and "0"), the signal in LTI mode shows longer charging and discharging time than that in DAM mode, thus producing a more distorted version of the intended PSK signal. RF data for other rates show similar characteristics but are not presented here.

Figure 4 shows an eye diagram of the measured, demodulated baseband signals overlaid with an ideal PSK signal passed through the same demodulation process. At lower data rates, e.g., $N = 10$, the eye is clearly visible for both LTI and DAM modes, though the LTI mode shows a longer charging and discharging envelope. When the data rate rises and greatly exceeds the antenna's bandwidth, the eye of the LTI system closes rapidly, becoming completely closed in the highest bandwidth ($N = 3$) case. Comparing the DAM performance to the LTI performance at the same rates, it is

1. Here we have simplified the timing description by assuming that N is an integer. Modification to the lag calculations for non-integer N is straightforward.

2. See [13] for the details of this process. Note that, unlike in [13], here the receive antenna response is also inverted and removed in the reported results.

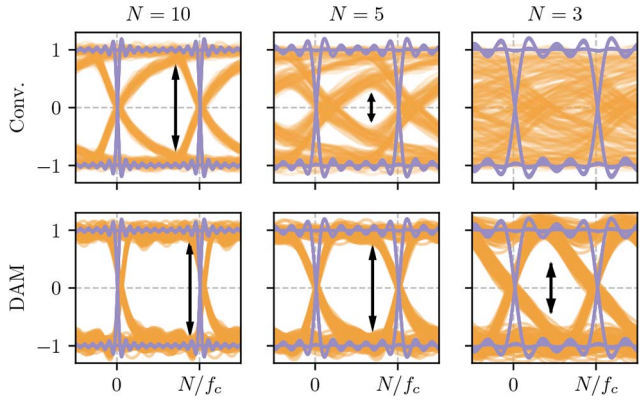

FIGURE 4. Measured (orange) and ideal (purple) BPSK eye diagrams at three data rates. The indicators in black show the widest eye-width position. Both DAM and conventional signals are normalized by the same factor.

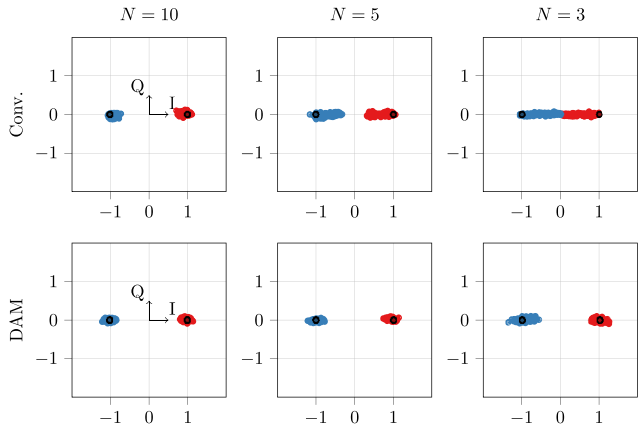

FIGURE 5. Measured BPSK constellations at three data rates. The two symbol states are plotted in different colors, while the ideal constellation points are shown in black.

evident that the DAM transmitter produces a much wider eye that remains distinguishable even the highest rate case.

The same data are plotted on a constellation diagram in Fig. 5 with sampling points chosen at the greatest average eye height indicated in Fig. 4. The ideal PSK constellation is shown in black. As expected, the distance between two pairs of symbol clusters are wide for both LTI and DAM modes at $N = 10$. As the data rate increases, the symbol clusters in LTI system begin to spread and the minimum distance between two pairs of symbol clusters decreases, indicating lower noise tolerance. In LTI mode, the constellation points of the two bits overlap in the highest data rate ($N = 3$), indicating that errors will arise from intersymbol interference (ISI) alone. However, in DAM mode, the two different symbols are widely separated even at high data rates.

In a second experiment, the same comparisons are made between DAM and LTI modes by transmitting a wideband quadrature PSK (QPSK, $M = 4$) signal. Figure 6 shows the constellation diagram of the measured signals. As the data rate increases, the symbol clusters (denoted by shaded convex hulls) produced by the LTI system spread out due to the narrowband nature of the transmit antenna and cause

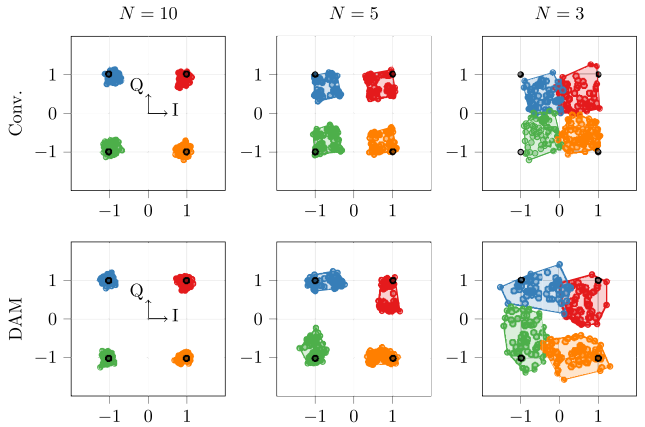

FIGURE 6. Measured QPSK constellations at three data rates. The four symbol states are plotted in different colors, while the ideal constellation points are shown in black.

TABLE 1. Error vector magnitude (EVM) in dB.

Modulation	N	Conv.	DAM
BPSK	10	-18	-20
	5	-6.7	-20
	3	0.53	-16
QPSK	10	-21	-20
	5	-9.5	-13
	3	-1.2	-3.7

different symbols to overlap at the highest data rate ($N = 3$). On the other hand, the DAM transmitter's constellations are more compact and show much less evidence of ISI with increasing data rate.

As a performance measure for the results shown in Figures 5 and 6, the error vector magnitude (EVM) relative to the center of each cluster is calculated in Table 1. As the data rate increases, the EVM of the conventional LTI mode increases dramatically in both BPSK and QPSK, while the EVM of the DAM mode in BPSK remains at nearly the same level. Comparing the QPSK results, it is clear that the QPSK DAM mode shows lower EVM than the LTI mode, however the relative gains are significantly lower than in the BPSK case. The reduced effectiveness of DAM for this QPSK demonstration is a result of parasitics in the transmitter switch, matching network and antenna [15]. While detailed study of these parasitic effects is beyond the scope of this work, ongoing study will elucidate the underlying sources of the degraded QPSK performance. Overall, these results are representative of the relative fidelity of the DAM and conventional transmitters irrespective of further signal processing that could be applied at the receiver.

C. DISTORTION AND EFFECTIVE BANDWIDTH ANALYSIS

Visual inspection of the time-domain waveforms, eye diagrams, and constellations in the previous section indicates the efficacy of DAM BPSK and QPSK in improving signal fidelity over a conventional transmitter. Here we quantify this improvement by comparison of the measured signals against an ideal PSK signal using distortion analysis [11], [16].

Defined as the distance between two signals under some fixed normalization and time alignment [16], distortion quantifies the fidelity with which an intended signal is reproduced by a transmitter over its entire duration at the RF level and provides an alternative to the pointwise, baseband metric plotted in constellation diagrams. For this analysis, the reference signal for distortion calculations is the ideal PSK waveform (e.g., that radiated by an ideal all-pass antenna) after being passed through the same noise-limiting bandpass filter used in over-the-air experiments. Because of the lead and lag periods in the proposed DAM PSK scheme, there is a difference between the ideal DAM PSK waveform and an ideal PSK signal. An asymptotic form of distortion for infinite random bit sequences produced by ideal DAM PSK with SSC may be derived by comparing the waveforms with lead and lag periods in Fig. 1 (DAM PSK with SSC) against those without (standard PSK) using the definition of distortion

$$d(x_1, x_2) = \int_{-\infty}^{\infty} |x_1(t) - x_2(t)|^2 \mathrm{d}t \tag{2}$$

where x_1 and x_2 are the properly normalized and time-aligned signals being compared. The resulting expression

$$d = 2\left(1 - \sqrt{1 - \frac{1}{N} + \frac{1}{MN}}\right) \tag{3}$$

shows the expected trend that this discrepancy becomes small for low data rate (large N) and is reduced at high data rates, particularly for low numbers of constellation points (low M). This expression provides a benchmark for the lowest distortion that is expected from an SSC DAM PSK system.

In Fig. 7, the measured receive signals studied in Section IV-B are compared to this benchmark and the calculated values of distortion are denoted by markers. Also shown is a model distortion curve (solid) for arbitrary data rates produced by passing the reference PSK signals through the bandpass filter represented by the measured receive antenna reflection coefficient. Additionally, we plot curves (dashed) denoting the predicted distortion for an ideal DAM transmitter with same-symbol correction (SSC) calculated via (3). Note that these ideal closed-form DAM reference curves do not include the effects of the bandpass filter applied to the received signals during channel inversion and are thus approximate for this particular scenario.

We observe excellent agreement between the measured conventional distortion and the model curve, with the expected trend of increasing distortion with increased data rate. For all measured data rates, the DAM BPSK and QPSK schemes produce significantly lower distortion than their LTI equivalents. In the case of DAM BPSK, distortion is reduced nearly to the value predicted for an ideal realized DAM waveform with SSC.

Using Fig. 7, the reduction in distortion observed in the DAM transmitter may be quantified in terms of effective bandwidth increase. For example, consider the case of $N = 3$ DAM BPSK. The measured distortion value of 0.19 could

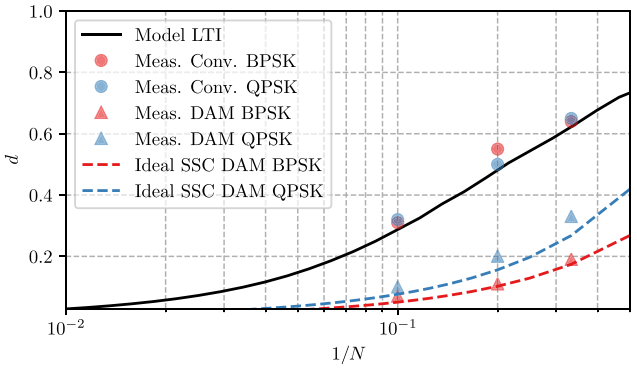

FIGURE 7. Measured QPSK and BPSK distortion compared against an LTI model of the transmitting antenna (solid) and ideal SSC DAM PSK as given by (3).

TABLE 2. Summary of effective bandwidth increases calculated for measured DAM PSK waveforms.

Modulation	N	N'	N'/N
BPSK	10	44	4.4
	5	28	5.6
	3	16	5.3
QPSK	10	29	2.9
	5	15	3.0
	3	8.1	2.7

only be achieved by the conventional transmitter by lowering the data rate to $N' = 16$, with this value being read off from the model conventional curve. Thus the bandwidth of the transmitted signals which may be transmitted for this value of distortion is effectively increased by a factor of 5.3 by moving from a conventional to DAM PSK transmitter. Similar calculations may be performed for all of the experimental trails and the resulting data are given in Tab. 2. Though distortion is not a one-to-one functional, this analysis provides quantification of the broadbanding effects of the proposed DAM PSK method.

V. EXTENSION TO HIGHER ORDER MODULATION

In principle, the DAM process presented in Section III is applicable to PSK of arbitrary order. In practice, however, realized performance in higher order DAM PSK is limited by switch properties such as off resistance, parasitic ringing effects, and on-off speed. Together, non-ideal switch properties such as these reduce the ability of the DAM transmitter to precisely capture and release energy for fast symbol transitions, thus degrading the fidelity of the transmitted waveform. These issues are likely to be exacerbated by higher order modulation schemes with closely spaced constellations. The experimental results in Section IV demonstrate this limitation in the relative fidelity of the DAM BPSK and DAM QPSK transmissions.

Nevertheless, technical challenges related to these circuit parasitics and switch non-idealities may be overcome in the future. In principle, the method proposed here is capable of producing broadband signals encoded with dense PSK constellations. As an example, simulation data are shown in Fig. 8 where a PSK constellation with 16 equally spaced

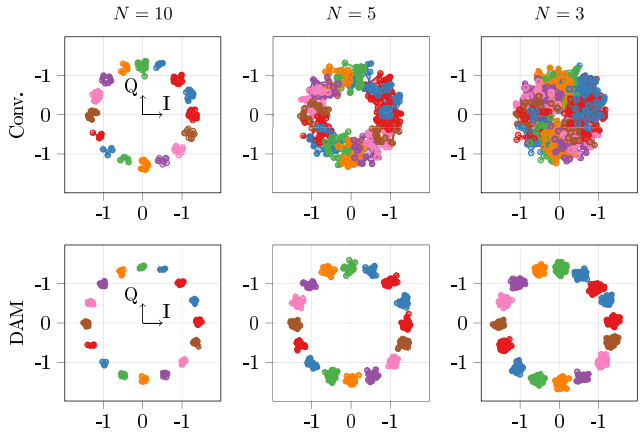

FIGURE 8. Simulated constellation diagrams of conventional and DAM 16-PSK transmitted by a system comparable to that used in experiment.

points is transmitted by a dipole antenna in conventional and DAM modes at varying data rates. The static -10 dB bandwidth of the simulated transmit antenna is 2.7% to approximate that of the antenna used in the experiments reported in Section IV. Transmitted waveforms are calculated using an equivalent circuit co-simulation method based on broadband models of dipole antennas [17]. Assuming ideal switch properties (lossless when closed, perfect isolation when open, instantaneous rise and fall times) and ideal matching network elements in this model, the relative advantage of DAM over the conventional transmitter is clearly observed even for this higher order PSK modulation.

Extension to modulation classes involving both amplitude and phase modulation (e.g., QAM) are not directly implementable using this method because the amplitude changes necessitate increases or decreases of stored energy on the antenna. However, implementing DAM versions of QAM-like modulation may be possible in the future using a combination of the binary amplitude control applied in DAM OOK [5], [13] and the phase control method presented here.

VI. CONCLUSION

A direct antenna modulation method for transmitting high data rate phase shift keyed signals using a narrowband electrically small dipole was described and experimentally validated. Measured results show that the DAM method transmits broadband PSK signals with greater fidelity than its conventional counterpart consisting of the same matching network and antenna. Distortion analysis indicates that the implemented DAM transmitter substantially increases $(2.7 - 5.6\times)$ the data rate at which BPSK and QPSK signals may be transmitted while maintaining distortion levels comparable to a conventional transmitter using the same narrowband antenna.

ACKNOWLEDGMENT

All statements of fact, opinion, or analysis expressed are those of the author and do not reflect the official positions or views of the Intelligence Community or any other U.S. Government agency. Nothing in the contents should be construed as asserting or implying U.S. Government authentication of information or endorsement of the authors' views.

REFERENCES

[1] L. J. Chu, "Physical limitations of omni-directional antennas," *J. Appl. Phys.*, vol. 19, pp. 1163–1175, Dec. 1948.

[2] K. P. Esselle and S. S. Stuchly, "Pulse-receiving characteristics of resistively loaded dipole antennas," *IEEE Trans. Antennas Propag.*, vol. 38, no. 10, pp. 1677–1683, Oct. 1990.

[3] K. Kim and W. R. Scott, "Design of a resistively loaded vee dipole for ultrawide-band ground-penetrating radar applications," *IEEE Trans. Antennas Propag.*, vol. 53, no. 8, pp. 2525–2532, Aug. 2005.

[4] H. Wolff, "High-speed frequency-shift keying of LF and VLF radio circuits," *IRE Transa. Commun. Syst.*, vol. 5, no. 3, pp. 29–42, Dec. 1957.

[5] J. Galejs, "Switching of reactive elements in high-Q antennas," *IEEE Trans. Commun. Syst.*, vol. CS-11, no. 2, pp. 254–255, Jun. 1963.

[6] X. Xu, H. C. Jing, and Y. E. Wang, "High speed pulse radiation from switched electrically small antennas," in *Proc. IEEE Antennas Propag. Soc. Int. Symp.*, 2006, pp. 167–170.

[7] M. Salehi, M. Manteghi, S.-Y. Suh, S. Sajuyigbe, and H. G. Skinner, "A wideband frequency-shift keying modulation technique using transient state of a small antenna," *Progress Electrom. Res.*, vol. 143, pp. 421–445, 2013. [Online]. Available: http://www.jpier.org/PIER/pier.php?paper=13102204

[8] R. Zhu and Y. E. Wang, "A modified QPSK modulation technique for direct antenna modulation (DAM) systems," in *Proc. IEEE Antennas Propag. Soc. Int. Symp. (APSURSI)*, 2014, pp. 1592–1593.

[9] A. D. Yaghjian and S. R. Best, "Impedance, bandwidth, and Q of antennas," *IEEE Trans. Antennas Propag.*, vol. 53, no. 4, pp. 1298–1324, Apr. 2005.

[10] M. Salehi and M. Manteghi, "Transient characteristics of small antennas," *IEEE Trans. Antennas Propag.*, vol. 62, no. 5, pp. 2418–2429, May 2014.

[11] K. Schab, A. Singh, and N. Bohannon, "Distortion analysis for the assessment of LTI and non-LTI transmitters," Jul. 2019. [Online]. Available: arXiv:1907.04354.

[12] X. J. Xu and Y. E. Wang, "A direct antenna modulation (DAM) transmitter with a switched electrically small antenna," in *Proc. Int. Workshop Antenna Technol. (iWAT)*, 2010, pp. 1–4.

[13] K. R. Schab, D. Huang, and J. J. Adams, "Pulse characteristics of a direct antenna modulation transmitter," *IEEE Access*, vol. 7, pp. 30213–30219, 2019.

[14] K. R. Schab and J. J. Adams, "Calculation of radiation transients in direct antenna modulation systems," in *Proc. IEEE Int. Symp. Antennas Propag. USNC/URSI Nat. Radio Sci. Meeting*, 2017, pp. 1–2.

[15] D. Huang, J. J. Adams, and K. Schab, "Ringing effects due to non-ideal components in direct antenna modulation transmitters," in *Proc. IEEE Int. Symp. Antennas Propag. USNC/URSI Nat. Radio Sci. Meeting*, Jul. 2019, pp. 1373–1374.

[16] D. Lamensdorf and L. Susman, "Baseband-pulse-antenna techniques," *IEEE Antennas Propag. Mag.*, vol. 36, no. 1, pp. 20–30, Feb. 1994.

[17] J. J. Adams and J. T. Bernhard, "Broadband equivalent circuit models for antenna impedances and fields using characteristic modes," *IEEE Trans. Antennas Propag.*, vol. 61, no. 8, pp. 3985–3994, Aug. 2013.